

Pion Interferometry of $\sqrt{s_{NN}} = 130$ GeV Au + Au Collisions at RHIC

C. Adler,¹¹ Z. Ahammed,²³ C. Allgower,¹² J. Amonett,¹⁴ B. D. Anderson,¹⁴ M. Anderson,⁵ G. S. Averichev,⁹ J. Balewski,¹² O. Barannikova,^{9,23} L. S. Barnby,¹⁴ J. Baudot,¹³ S. Bekele,²⁰ V. V. Belaga,⁹ R. Bellwied,³⁰ J. Berger,¹¹ H. Bichsel,²⁹ L. C. Bland,¹² C. O. Blyth,³ B. E. Bonner,²⁴ R. Bossingham,¹⁵ A. Boucham,²⁶ A. Brandin,¹⁸ R. V. Cadman,¹ H. Caines,²⁰ M. Calderón de la Barca Sánchez,³¹ A. Cardenas,²³ J. Carroll,¹⁵ J. Castillo,²⁶ M. Castro,³⁰ D. Cebra,⁵ S. Chattopadhyay,³⁰ M. L. Chen,² Y. Chen,⁶ S. P. Chernenko,⁹ M. Cherney,⁸ A. Chikanian,³¹ B. Choi,²⁷ W. Christie,² J. P. Coffin,¹³ L. Conin,²⁶ T. M. Cormier,³⁰ J. G. Cramer,²⁹ H. J. Crawford,⁴ M. DeMello,²⁴ W. S. Deng,¹⁴ A. A. Derevschikov,²² L. Didenko,² J. E. Draper,⁵ V. B. Dunin,⁹ J. C. Dunlop,³¹ V. Eckardt,¹⁶ L. G. Efimov,⁹ V. Emelianov,¹⁸ J. Engelage,⁴ G. Eppley,²⁴ B. Erazmus,²⁶ P. Fachini,²⁵ V. Faine,² E. Finch,³¹ Y. Fisyak,² D. Flierl,¹¹ K. J. Foley,² J. Fu,¹⁵ N. Gagunashvili,⁹ J. Gans,³¹ L. Gaudichet,²⁶ M. Germain,¹³ F. Geurts,²⁴ V. Ghazikhanian,⁶ J. Grabski,²⁸ O. Grachov,³⁰ D. Greiner,¹⁵ V. Grigoriev,¹⁸ M. Guedon,¹³ E. Gushin,¹⁸ T. J. Hallman,² D. Hardtke,¹⁵ J. W. Harris,³¹ M. Heffner,⁵ S. Heppelmann,²¹ T. Herston,²³ B. Hippolyte,¹³ A. Hirsch,²³ E. Hjort,¹⁵ G. W. Hoffmann,²⁷ M. Horsley,³¹ H. Z. Huang,⁶ T. J. Humanic,²⁰ H. Hümmeler,¹⁶ G. Igo,⁶ A. Ishihara,²⁷ Yu. I. Ivanshin,¹⁰ P. Jacobs,¹⁵ W. W. Jacobs,¹² M. Janik,²⁸ I. Johnson,¹⁵ P. G. Jones,³ E. Judd,⁴ M. Kaneta,¹⁵ M. Kaplan,⁷ D. Keane,¹⁴ A. Kisiel,²⁸ J. Klay,⁵ S. R. Klein,¹⁵ A. Klyachko,¹² A. S. Konstantinov,²² L. Kotchenda,¹⁸ A. D. Kovalenko,⁹ M. Kramer,¹⁹ P. Kravtsov,¹⁸ K. Krueger,¹ C. Kuhn,¹³ A. I. Kulikov,⁹ G. J. Kunde,³¹ C. L. Kunz,⁷ R. Kh. Kutuev,¹⁰ A. A. Kuznetsov,⁹ L. Lakehal-Ayat,²⁶ J. Lamas-Valverde,²⁴ M. A. C. Lamont,³ J. M. Landgraf,² S. Lange,¹¹ C. P. Lansdell,²⁷ B. Lasiuk,³¹ F. Laue,² A. Lebedev,² T. LeCompte,¹ R. Lednický,⁹ V. M. Leontiev,²² M. J. LeVine,² Q. Li,³⁰ Q. Li,¹⁵ S. J. Lindenbaum,¹⁹ M. A. Lisa,²⁰ T. Ljubicic,² W. J. Llope,²⁴ G. LoCurto,¹⁶ H. Long,⁶ R. S. Longacre,² M. Lopez-Noriega,²⁰ W. A. Love,² D. Lynn,² R. Majka,³¹ S. Margetis,¹⁴ L. Martin,²⁶ J. Marx,¹⁵ H. S. Matis,¹⁵ Yu. A. Matulenko,²² T. S. McShane,⁸ F. Meissner,¹⁵ Yu. Melnick,²² A. Meschanin,²² M. Messer,² M. L. Miller,³¹ Z. Milosevich,⁷ N. G. Minaev,²² J. Mitchell,²⁴ V. A. Moiseenko,¹⁰ D. Moltz,¹⁵ C. F. Moore,²⁷ V. Morozov,¹⁵ M. M. de Moura,³⁰ M. G. Munhoz,²⁵ G. S. Mutchler,²⁴ J. M. Nelson,³ P. Nevski,² V. A. Nikitin,¹⁰ L. V. Nogach,²² B. Norman,¹⁴ S. B. Nurushev,²² G. Odyniec,¹⁵ A. Ogawa,²¹ V. Okorokov,¹⁸ M. Oldenburg,¹⁶ D. Olson,¹⁵ G. Paic,²⁰ S. U. Pandey,³⁰ Y. Panebratsev,⁹ S. Y. Panitkin,² A. I. Pavlinov,³⁰ T. Pawlak,²⁸ V. Perevoztchikov,² W. Peryt,²⁸ V. A. Petrov,¹⁰ W. Pinganaud,²⁶ E. Platner,²⁴ J. Pluta,²⁸ N. Porile,²³ J. Porter,² A. M. Poskanzer,¹⁵ E. Potrebenikova,⁹ D. Prindle,²⁹ C. Pruneau,³⁰ S. Radomski,²⁸ G. Rai,¹⁵ O. Ravel,²⁶ R. L. Ray,²⁷ S. V. Razin,^{9,12} D. Reichhold,⁸ J. G. Reid,²⁹ F. Retiere,¹⁵ A. Ridiger,¹⁸ H. G. Ritter,¹⁵ J. B. Roberts,²⁴ O. V. Rogachevski,⁹ J. L. Romero,⁵ C. Roy,²⁶ D. Russ,⁷ V. Rykov,³⁰ I. Sakrejda,¹⁵ J. Sandweiss,³¹ A. C. Saulys,² I. Savin,¹⁰ J. Schambach,²⁷ R. P. Scharenberg,²³ K. Schweda,¹⁵ N. Schmitz,¹⁶ L. S. Schroeder,¹⁵ A. Schüttauf,¹⁶ J. Seger,⁸ D. Seliverstov,¹⁸ P. Seyboth,¹⁶ E. Shahaliev,⁹ K. E. Shestermanov,²² S. S. Shimanskii,⁹ V. S. Shvetsov,¹⁰ G. Skoro,⁹ N. Smirnov,³¹ R. Snellings,¹⁵ J. Sowinski,¹² H. M. Spinka,¹ B. Srivastava,²³ E. J. Stephenson,¹² R. Stock,¹¹ A. Stolpovsky,³⁰ M. Strikhanov,¹⁸ B. Stringfellow,²³ H. Stroebele,¹¹ C. Struck,¹¹ A. A. P. Suaide,³⁰ E. Sugarbaker,²⁰ C. Suire,¹³ M. Šumbera,⁹ T. J. M. Symons,¹⁵ A. Szanto de Toledo,²⁵ P. Szarwas,²⁸ J. Takahashi,²⁵ A. H. Tang,¹⁴ J. H. Thomas,¹⁵ V. Tikhomirov,¹⁸ T. A. Trainor,²⁹ S. Trentalange,⁶ M. Tokarev,⁹ M. B. Tonjes,¹⁷ V. Trofimov,¹⁸ O. Tsai,⁶ K. Turner,² T. Ullrich,² D. G. Underwood,¹ G. Van Buren,² A. M. VanderMolen,¹⁷ A. Vanyashin,¹⁵ I. M. Vasilevski,¹⁰ A. N. Vasiliev,²² S. E. Vigdor,¹² S. A. Voloshin,³⁰ F. Wang,²³ H. Ward,²⁷ J. W. Watson,¹⁴ R. Wells,²⁰ T. Wenaus,² G. D. Westfall,¹⁷ C. Whitten, Jr.,⁶ H. Wieman,¹⁵ R. Willson,²⁰ S. W. Wissink,¹² R. Witt,¹⁴ N. Xu,¹⁵ Z. Xu,³¹ A. E. Yakutin,²² E. Yamamoto,⁶ J. Yang,⁶ P. Yepes,²⁴ A. Yokosawa,¹ V. I. Yurevich,⁹ Y. V. Zanevski,⁹ I. Zborovský,⁹ W. M. Zhang,¹⁴ R. Zoulkarneev,¹⁰ and A. N. Zubarev⁹

(STAR Collaboration)

¹Argonne National Laboratory, Argonne, Illinois 60439

²Brookhaven National Laboratory, Upton, New York 11973

³University of Birmingham, Birmingham, United Kingdom

⁴University of California, Berkeley, California 94720

⁵University of California, Davis, California 95616

⁶University of California, Los Angeles, California 90095

⁷Carnegie Mellon University, Pittsburgh, Pennsylvania 15213

⁸Creighton University, Omaha, Nebraska 68178

⁹Laboratory for High Energy (JINR), Dubna, Russia

¹⁰Particle Physics Laboratory (JINR), Dubna, Russia

- ¹¹University of Frankfurt, Frankfurt, Germany
¹²Indiana University, Bloomington, Indiana 47408
¹³Institut de Recherches Subatomiques, Strasbourg, France
¹⁴Kent State University, Kent, Ohio 44242
¹⁵Lawrence Berkeley National Laboratory, Berkeley, California 94720
¹⁶Max-Planck-Institut fuer Physik, Munich, Germany
¹⁷Michigan State University, East Lansing, Michigan 48824
¹⁸Moscow Engineering Physics Institute, Moscow, Russia
¹⁹City College of New York, New York, New York 10031
²⁰Ohio State University, Columbus, Ohio 43210
²¹Pennsylvania State University, University Park, Pennsylvania 16802
²²Institute of High Energy Physics, Protvino, Russia
²³Purdue University, West Lafayette, Indiana 47907
²⁴Rice University, Houston, Texas 77251
²⁵Universidade de Sao Paulo, Sao Paulo, Brazil
²⁶SUBATECH, Nantes, France
²⁷University of Texas, Austin, Texas 78712
²⁸Warsaw University of Technology, Warsaw, Poland
²⁹University of Washington, Seattle, Washington 98195
³⁰Wayne State University, Detroit, Michigan 48201
³¹Yale University, New Haven, Connecticut 06520
(Received 9 May 2001; published 3 August 2001)

Two-pion correlation functions in Au + Au collisions at $\sqrt{s_{NN}} = 130$ GeV have been measured by the STAR (solenoidal tracker at RHIC) detector. The source size extracted by fitting the correlations grows with event multiplicity and decreases with transverse momentum. Anomalously large sizes or emission durations, which have been suggested as signals of quark-gluon plasma formation and rehadronization, are not observed. The Hanbury Brown–Twiss parameters display a weak energy dependence over a broad range in $\sqrt{s_{NN}}$.

DOI: 10.1103/PhysRevLett.87.082301

PACS numbers: 25.75.Gz, 25.75.Ld

Two-particle intensity interferometry techniques [Hanbury Brown–Twiss (HBT)] have been used extensively to probe the space-time structure of heavy ion collisions [1]. At midrapidity ($y = 0$) and low transverse momentum (p_T), two-pion correlation functions reflect the space-time geometry of the emitting source, while dynamical information (e.g., collective flow) is contained in the momentum dependence of the apparent source size [2–4].

In this Letter we study two-pion correlation functions in Au + Au collisions at nucleon-nucleon center-of-mass energy $\sqrt{s_{NN}} = 130$ GeV produced by the RHIC facility at Brookhaven National Laboratory, and compare our results to similar studies at lower energy. Such systematic comparisons may reveal the onset of new phenomena, as $\sqrt{s_{NN}}$ increases. We are particularly interested in possible indications that a quark gluon plasma (QGP) has been formed in the collision. Several authors [1,4–8] have proposed HBT studies to probe for a significant increase in the pion emission time scale associated with QGP formation.

Experimentally, the two-particle correlation function is obtained from the ratio $C_2(\mathbf{q}) = A(\mathbf{q})/B(\mathbf{q})$ (normalized to unity at large \mathbf{q}), where $A(\mathbf{q})$ is the measured two-pion distribution of pair momentum difference $\mathbf{q} = \mathbf{p}_2 - \mathbf{p}_1$, and $B(\mathbf{q})$ is the mixed background distribution [9], calculated in the same way by using pairs of particles taken from different events.

The STAR time projection chamber (TPC) [10,11] was used to record charged particle tracks as they crossed

up to 45 pad rows of the detector. For P-10 gas in the 0.25 T solenoidal magnetic field, transverse and longitudinal diffusion were both about 350 μm times the square root of the drift length. The TPC was read out with 138 000 waveform digitizer channels [12]; the signal shaping width was comparable to the diffusion. For a typical 1.5 m drift, two-track resolution was limited by the resulting 6 mm signal spread, in addition to geometric spreading due to tracks traversing the pad rows at finite crossing angles. This analysis used tracks with $0.125 < p_T < 0.45$ GeV/ c and $|y| < 0.5$, for which the reconstruction and π identification efficiencies are high. We present results for three p_T ranges: 0.125–0.225 GeV/ c , 0.225–0.325 GeV/ c , and 0.325–0.45 GeV/ c .

We select events with a collision position that is within 75 cm of the midplane of the 4-m-long TPC. An important feature of two-particle correlation functions is that single-particle phase space and acceptance effects cancel to first order. To preserve this feature in the collider environment (in which the collision vertex—and hence the single-particle acceptance—varies event-to-event), we only mix events which have a primary vertex longitudinal location within 15 cm of each other; however, mixing events over the full ± 75 cm range introduces no significant distortion in the correlation fit parameters, in the present analysis.

Starting with a minimum-bias trigger [13], we characterize the centrality of collisions off-line according to the

measured multiplicity of negatively charged particles with pseudorapidity $|\eta| < 0.5$. After accounting for event reconstruction inefficiency for low-multiplicity events, we estimate that the minimum-bias distribution contains $\sim 90\%$ of the hadronic Au + Au cross section [13]. We analyze $\sim 10^5$ events in each of the three bins; bin 3 contains the 12% most central of the measured collisions, bin 2 contains the next 20%, and bin 1 contains the next 40%.

Particle identification was achieved by correlating the magnetic rigidity of a track with its specific ionization (dE/dx) in the gas of the TPC. In the momentum region of interest, π , K , and p/\bar{p} are well separated; contamination of the pion sample by electrons is the primary concern. Based on simulations and on extrapolation from regions of clear e^-/π^- separation, we estimate that electrons comprise about 10% (4%) of the selected tracks in our lowest (highest) p_T bin. Tracks used in the correlations are required to project back to the primary interaction vertex within 3 cm, thereby selecting primarily pions emitted directly from the collision. Contamination from nonpions and pions originating from long-lived decays (e.g., Λ , ω) reduces the strength of the correlation, characterized by the parameter λ , while leaving the extracted source radii unchanged [14,15].

Although track splitting (incorrect reconstruction of a single particle as two particles) in the STAR TPC is a small effect in general ($\leq 1\%$), it may have a strong impact on correlation studies at low $|q|$. False pairs generated by track splitting are removed by a topological cut which requires valid and distinct signals of both tracks on several TPC pad rows. For the present analysis, residual effects of track splitting are negligible.

To eliminate the effect of track merging (in which two tracks with similar momenta are reconstructed as a single track), we require the tracks in a pair to be well separated (> 2.5 cm at the radius of the TPC inner field cage, 50 cm). In applying this cut also to the mixed-pair background, the effect of event-to-event variation in the primary vertex position is taken into account. The antimerging cut removes significant detector effects, but also discriminates against low- $|q|$ pairs, which carry the correlation signal. This leads to an artificial reduction in the HBT parameters, which we estimate, based on simulations [16], to be 3%–6% for the radii and 6%–14% for λ , depending on p_T . We correct for this effect in the results presented.

We apply to each background pair a Coulomb correction [4] corresponding to a spherical Gaussian source of 5 fm radius; this correction is identical to that used by several other groups [14,20,21]. In principle, this procedure over-corrects the correlation function for realistic sources (e.g., in which some pions originate far from the core source). We find that the HBT radii change smoothly by $\sim 10\%$ as the strength of the Coulomb correction is varied from the standard correction to no correction. Here, we restrict ourselves to the standard Coulomb correction, allowing for a uniform extension of existing interferometry systematics from lower energy.

One-dimensional (1D) correlation functions constructed in the invariant quantity $Q_{\text{inv}} = \sqrt{(\mathbf{p}_1 - \mathbf{p}_2)^2 - (E_1 - E_2)^2}$ are fit to the functional form

$$C(Q_{\text{inv}}) = 1 + \lambda \exp(-Q_{\text{inv}}^2 R_{\text{inv}}^2). \quad (1)$$

The 1D correlation function (and fit) corresponding to our highest multiplicity class is shown in Fig. 1a for low- p_T π^- . The one-dimensional fit fails in lowest Q_{inv} bins, as was observed in previous measurements [22,23]. Hence, the extracted radius $R_{\text{inv}} \approx 6.3$ fm is only a rough indication of the space-time extent of the source.

A more detailed characterization of the emitting source is obtained through multidimensional correlation functions. We decompose the momentum difference \mathbf{q} according to the Pratt-Bertsch [4,7] “out-side-long” (indicated by o , s , and l subscripts) parametrization. Here, q_l is parallel to the beam, q_s is perpendicular to the beam and to the total momentum of the pair, and q_o is perpendicular to q_l and q_s . Data are analyzed in the longitudinally comoving system frame, in which the longitudinal component of the pair momentum vanishes. Figures 1b–1d show one-dimensional projections of the correlation function $C(q_o, q_s, q_l)$ onto the q_o , q_s , and q_l axes, for π^- from the most central collisions.

The three-dimensional correlation functions are fit with the standard Gaussian form

$$C(q_o, q_s, q_l) = 1 + \lambda \exp(-R_o^2 q_o^2 - R_s^2 q_s^2 - R_l^2 q_l^2), \quad (2)$$

where R_i is the homogeneity length in the i direction [1].

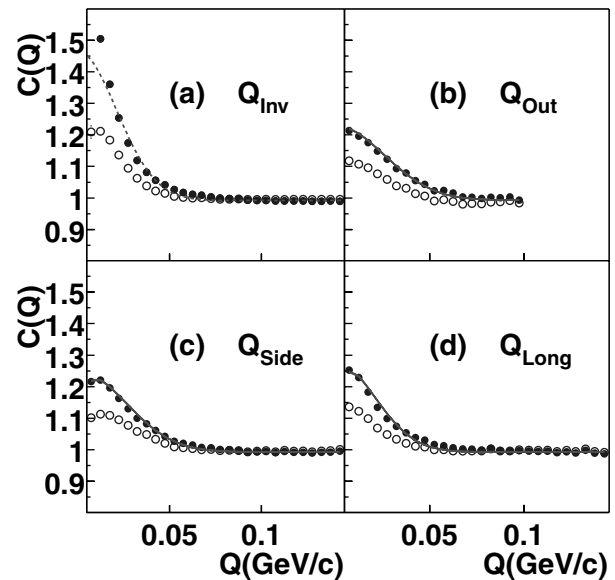


FIG. 1. Coulomb-corrected (filled circles) and -uncorrected (open circles) correlation functions for low- p_T π^- emitted at midrapidity from central collisions. Shown in panel (a) is the Q_{inv} correlation function, and panels (b)–(d) show projections of the three-dimensional correlation function onto the q_o , q_s , and q_l axes. To project onto one q component, the others are integrated over the range 0–35 MeV/c. Fits to Coulomb-corrected correlations are shown by curves.

Projections of the fit to the central collisions, weighted according to the mixed-pair background, are shown as curves in Fig. 1.

Systematic errors on the HBT fit parameters have two sources of roughly equal magnitude: (i) the uncertainty on the correction for the antimerging cut, estimated equal to the correction itself, and (ii) the uncertainty associated with the Coulomb correction, $\sim 0.1\text{--}0.2$ fm in the radii, determined by varying the Coulomb radius by ± 1 fm.

The effect of the single-particle momentum resolution ($\delta p/p \sim 2\%$ in the TPC for the particles under study) is known to induce systematic underestimates of HBT parameters. For our lowest p_T bin, $\delta q_o \approx 4.5$ MeV/c, and $\delta q_s \approx \delta q_l \approx 3$ MeV/c. While δq_s and δq_l change little, in our highest p_T bin, $\delta q_o \approx 11$ MeV/c. Using an iterative procedure similar to that used at lower energies [14,22], we have corrected our correlation functions for finite resolution effects. The correction had no effect on the HBT parameters for our lowest p_T cut; for the highest p_T cut, it resulted in a 5% increase in λ and a 8% increase in R_o , while R_s and R_l were unaffected.

The multiplicity dependence of the source parameters is presented in the left panels of Fig. 2, for low- p_T , midrapidity $\pi^-\pi^-$ and $\pi^+\pi^+$ correlations. The parameters for positive and negative pions are similar; the λ parameter is constant, and all three radii increase monotonically with multiplicity. The increase of the transverse radii R_o and R_s with multiplicity is interpreted as a geometrical effect, and is also observed in lower energy measurements [14,24,25]. The multiplicity dependence of R_l differs from observations at lower energies; E895 [14] and NA49 [25]

observe no dependence of R_l over a wide range of multiplicity at the Alternating Gradient Synchrotron (AGS) and CERN Super Proton Synchrotron (SPS), while NA44 [26] reports a sharp increase for the very highest multiplicity collisions at the SPS.

The right panels of Fig. 2 show, for the events in multiplicity bin 3, the dependence of the HBT parameters on $m_T = \sqrt{p_T^2 + m^2}$. λ increases with m_T , consistent with studies at lower energy [14,22,23], in which the increase was attributed to decreased contributions of pions from long-lived resonances at higher p_T .

The radius parameters decrease significantly with m_T . This m_T dependence, weak at $\sqrt{s_{NN}} \sim 2$ GeV [14] and growing stronger with collision energy [22–24,27], reflects pion emission from a radially expanding source [1]. The m_T dependence at RHIC is similar, but not identical, to that observed in central Pb + Pb collisions at the SPS [22,23,27]. The significant decrease of R_o with m_T contrasts with the m_T independence of R_o measured at midrapidity in collisions at SPS energy [23,27]. For our highest m_T data, $R_o < R_s$, possibly indicating significant source opacity resulting from the high-particle densities generated in RHIC collisions [28,29].

To place our results in context, Fig. 3 shows the world's data set of correlation parameters for midrapidity, low- p_T (~ 170 MeV/c) π^- from central Au + Au or Pb + Pb collisions. The parameter λ falls smoothly and rapidly from unity (the expected value from naive assumptions), at $\sqrt{s_{NN}} \sim 2$ GeV, to about 0.5 at RHIC; this decrease is attributed partially to an increased fraction of π^- arising from long-lived decays as $\sqrt{s_{NN}}$ increases [14,30]. Since λ is also affected by several experiment-specific effects (e.g., e^- rejection efficiency), we do not focus on the details of its excitation function.

The radius parameter R_s correlates most directly with source geometry [1]. After an initial decrease at AGS energies, attributed to increasing space-momentum correlations [14], R_s appears to rise slightly with collision energy, reflecting a larger freeze-out volume with increasing pion multiplicity. Similarly, R_l does not exhibit a large increase with collision energy, after the initial increase between AGS and SPS energies.

The parameter R_o encodes both geometry and time scale information; in the absence of flow and opacity effects, the emission time scale (duration of freeze-out) is given by $\tau = \sqrt{R_o^2 - R_s^2}/\beta_T$, where β_T is the average transverse velocity of a pion pair. Both R_o and $\sqrt{R_o^2 - R_s^2}$ are relatively independent of energy; we see no evidence for a large increase in the emission time scale (e.g., due to QGP formation [5]).

In hydrodynamic models [5,6], the ratio R_o/R_s is a sensitive probe of the equation of state. In a purely hadronic (non-QGP) scenario, $R_o/R_s \approx 1.0\text{--}1.2$, while formation of QGP is predicted to produce $R_o/R_s \approx 1.5\text{--}10$. This ratio, plotted in the bottom panel of Fig. 3 for low- p_T pions, does not show a significant rise at RHIC. Furthermore, at RHIC, R_o/R_s is observed to decrease (from 1.07 to 0.89)

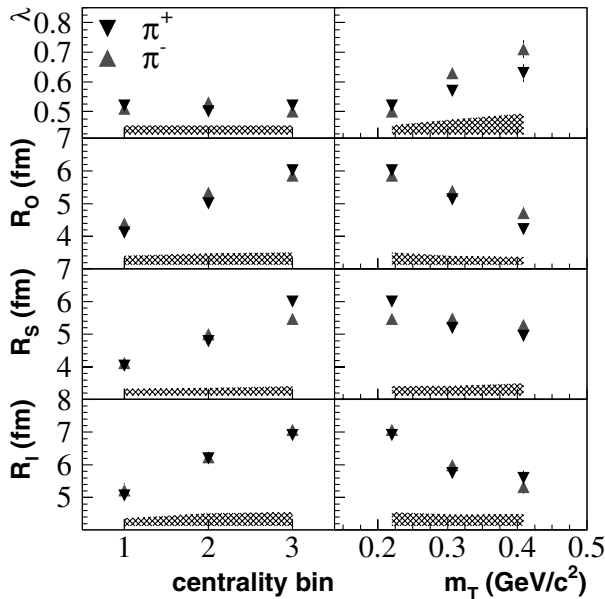


FIG. 2. The multiplicity dependence of the HBT parameters is shown for low- p_T pions on the left; bin 3 contains the high-multiplicity events. For high-multiplicity collisions, the m_T dependences are shown on the right. The error bars indicate statistical uncertainties; systematic uncertainties are represented by the height of the shaded regions below.

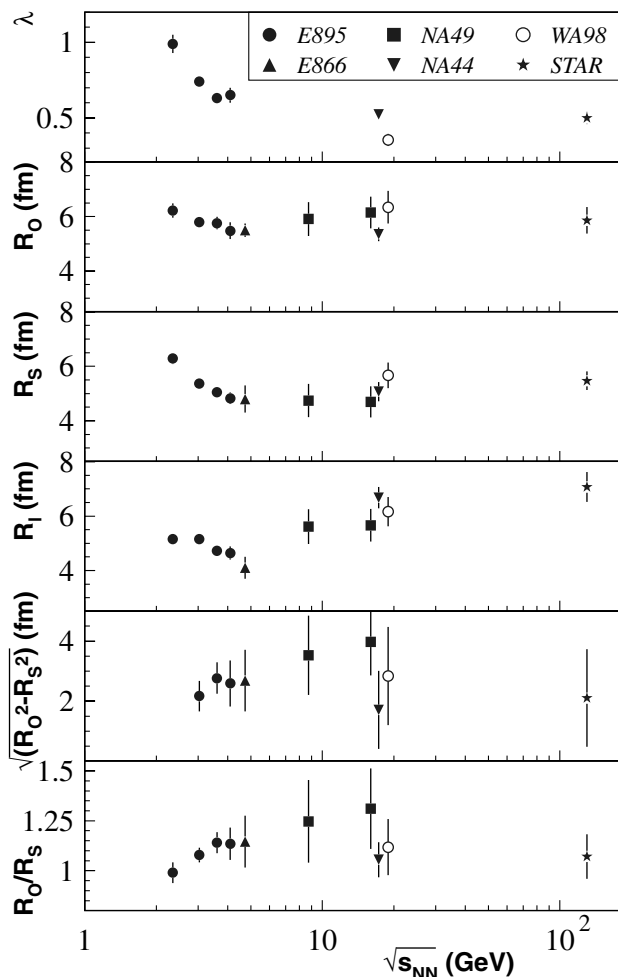


FIG. 3. The energy dependence of π^- HBT parameters for central Au + Au (Pb + Pb) collisions at midrapidity and $p_T \approx 0.17$ GeV/c [14,22–24,27]. The SPS data are offset slightly in $\sqrt{s_{NN}}$ for clarity. Error bars on NA44, NA49, and STAR results include systematic uncertainties; error bars on other results are statistical.

with p_T , in contrast to recent transport calculations [31] which include the effects of hadronic rescattering after a hydrodynamic stage with a QGP phase. We note, however, that the long emission duration QGP signature is expected [6] to vanish again at energies higher than its onset, due to rapid expansion of the system. Because of the large energy difference between SPS and RHIC, without intervening measurements, we cannot rule out an increase in the emission time scale at some lower, intermediate energy.

In conclusion, STAR has measured two-pion correlation functions in Au + Au collisions at $\sqrt{s_{NN}} = 130$ GeV. Transverse HBT radii grow with event multiplicity, reflecting the evolution of source geometry with centrality. In contrast to studies at lower energies, R_l also increases steadily over a large range of multiplicities; more study is required to understand the origin of this effect. The m_T dependence of the HBT radii is stronger than at lower energies, suggesting emission from a more rapidly expanding source at RHIC, and, in particular, the much stronger decrease in R_o at high m_T may indicate the onset

of opaqueness in the dense system. The pion interferometry excitation function for the heaviest ions now spans nearly two decades in $\sqrt{s_{NN}}$. No sudden jumps in HBT radii are observed, but lower energy RHIC measurements are needed to complete the search for a predicted increase in emission time scale related to the possible onset of QGP formation.

We thank the RHIC Operations Group at Brookhaven National Laboratory for their tremendous support and for providing collisions for the experiment. This work was supported by the Division of Nuclear Physics and the Division of High Energy Physics of the Office of Science of the U.S. Department of Energy, the United States National Science Foundation, the Bundesministerium fuer Bildung und Forschung of Germany, the Institut National de la Physique Nucleaire et de la Physique des Particules of France, the United Kingdom Engineering and Physical Sciences Research Council, Fundacao de Amparo a Pesquisa do Estado de Sao Paulo, Brazil, and the Russian Ministry of Science and Technology.

- [1] W. Bauer, C.K. Gelbke, and S. Pratt, *Annu. Rev. Nucl. Part. Sci.* **42**, 77 (1992); U. Heinz and B. Jacak, *Annu. Rev. Nucl. Part. Sci.* **49**, 529 (1999); U.A. Wiedemann and U. Heinz, *Phys. Rep.* **319**, 145 (1999).
- [2] S. Pratt, *Phys. Rev. Lett.* **53**, 1219 (1984).
- [3] A.N. Makhlin and Y.M. Sinyukov, *Z. Phys. C* **39**, 69 (1988).
- [4] S. Pratt, T. Csörgö, and J. Zimanyi, *Phys. Rev. C* **42**, 2646 (1990).
- [5] D.H. Rischke, *Nucl. Phys.* **A610**, 88c (1996).
- [6] D.H. Rischke and M. Gyulassy, *Nucl. Phys.* **A608**, 479 (1996).
- [7] G. Bertsch, M. Gong, and M. Tohyama, *Phys. Rev. C* **37**, 1896 (1988); G. Bertsch, *Nucl. Phys.* **A498**, 173c (1989).
- [8] C.M. Hung and E.V. Shuryak, *Phys. Rev. Lett.* **75**, 4003 (1995).
- [9] G.I. Kopylov, *Phys. Lett.* **50B**, 472 (1974).
- [10] STAR Collaboration, K.H. Ackermann *et al.*, *Nucl. Phys.* **A661**, 681c (1999).
- [11] H. Wieman *et al.*, *IEEE Trans. Nucl. Sci.* **44**, 671 (1997).
- [12] W. Betts *et al.*, *IEEE Trans. Nucl. Sci.* **44**, 592 (1997); S. Klein *et al.*, *IEEE Trans. Nucl. Sci.* **43**, 1768 (1996).
- [13] STAR Collaboration, K.H. Ackermann *et al.*, *Phys. Rev. Lett.* **86**, 402 (2001).
- [14] E895 Collaboration, M.A. Lisa *et al.*, *Phys. Rev. Lett.* **84**, 2798 (2000); *Nucl. Phys.* **A661**, 444c (1999).
- [15] H. Appelshäuser, Ph.D. thesis, University of Frankfurt, 1996.
- [16] We note that, in order to faithfully reproduce the effect of the antimerger cut on the parameters from a Gaussian fit to the experimental correlation function, we needed to assume a slightly non-Gaussian source distribution in our simulations; assuming a purely Gaussian distribution leads to a much weaker effect than is observed. In realistic transport calculations [17,18] such non-Gaussian distributions are generated by dynamic expansion [19] and “halo” emission from long-lived resonances.

- [17] T. J. Humanic, Phys. Rev. C **57**, 866 (1998).
[18] H. Sorge, Phys. Rev. C **52**, 3291 (1995).
[19] D. Hardtke and S. A. Voloshin, Phys. Rev. C **61**, 024905 (2000).
[20] E877 Collaboration, J. Barrette *et al.*, Nucl. Phys. **A610**, 227c (1996); Phys. Rev. Lett. **78**, 2916 (1997).
[21] NA49 Collaboration, K. Kadija *et al.*, Nucl. Phys. **A610**, 248c (1996).
[22] NA44 Collaboration I. G. Bearden *et al.*, Phys. Rev. C **58**, 1656 (1998).
[23] WA98 Collaboration, M. M. Aggarwal *et al.*, Eur. Phys. J. C **16**, 445 (2000).
[24] E866 Collaboration, R. Soltz *et al.*, Nucl. Phys. **A661**, 439c (1999).
[25] NA49 Collaboration, R. Ganz *et al.*, Nucl. Phys. **A661**, 448c (1999).
[26] NA44 Collaboration, I. G. Bearden *et al.*, Eur. Phys. J. C **18**, 317 (2000).
[27] NA49 Collaboration, C. Blume *et al.*, Proceedings of the International Conference on Quark Matter 2001 (to be published).
[28] H. Heiselberg and A. P. Vischer, Eur. Phys. J. C **1**, 593 (1998).
[29] B. Tomášik and U. Heinz, nucl-th/9805016.
[30] J. Sullivan *et al.*, Nucl. Phys. **A566**, 531c (1994).
[31] S. Soff, S. Bass, and A. Dumitru, Phys. Rev. Lett. **86**, 3981 (2001).